Soft Matter

COMMUNICATION

View Article Online
View Journal | View Issue

Cite this: *Soft Matter*, 2019, **15**, 5815

Received 25th May 2019,
Accepted 3rd July 2019

DOI: 10.1039/c9sm01051c

rsc.li/soft-matter-journal

Measurement of the force between uncharged colloidal particles trapped at a flat air/water interface†

Virginia Carrasco-Fadanelli and Rolando Castillo *

The radial attraction between microspheres straddling at the air/water interface (Bond number $\ll 1$), whose origin is the irregular shape of the contact line and its concomitant distortion of the water surface, is measured using two light beams of a time-sharing optical tweezer. The colloidal particles used to make the measurements are microspheres made of hydrophobically covered silica to reduce the electrostatic interactions to a minimum. The measured radial force goes as a quadrupolar power law, r^{-n}, with $n = 5.02 \pm 0.18$ and $n = 5.04 \pm 0.18$ for particles of 3 μm and 5 μm, respectively. In both cases, the electrostatic interaction is negligible.

More than 35 years ago, de Gennes[1,2] suggested that the solid–liquid–vapor contact line must have an irregular shape to explain the contact angle hysteresis in partial wetting, because of the pinning of this line on nanoscopic sites due to roughness or chemical heterogeneities on the solid surface.

The anchorage of the triple line on defects of the solid surface and its dynamics have significant consequences in the behavior of colloidal particles trapped at interfaces. Free energy traps colloids irreversibly at interfaces. When gravity is not playing a role, Bond number (capillarity length/particle radius) $\ll 1$, the interface where colloidal particles are trapped is not deformed, and if the particle is in equilibrium, the contact angle given by Young's law, in principle, entirely determines it flotation level. However, the interface close around the particles can still be deformed due to the irregular shape of the contact line, also pinned on nanoscopic sites on the colloid surface. Therefore, particles trapped on a planar interface can strongly interact to lower surface energy, even when they are not charged.

Stamou *et al.*[3] theoretically derived a lateral attraction between homogeneous uncharged microparticles trapped at the air/water (A/W) interface, whose origin is the irregular shape of the contact line and its concomitant distortion of the water surface. Capillary interaction occurs between particles as they move to minimize the interfacial area. The most relevant term of the interaction potential found by these authors and by others[4] is:

$$V(r) = -12\pi\gamma {H_2}^2 \cos[2(\varphi_A + \varphi_B)](r_c/r)^4, \quad (1)$$

where the sphere and the water surface intersect at the average contact radius r_c, and r is the center-to-center distance between spheres. H_2 is the height of the meniscus at the contact line, γ is the liquid surface tension, the φ_i are orientation angles of particles (A and B) relative to a line joining their centers. Therefore, when interface deformations of neighboring particles overlap, particles rotate and approach each other, and assemble to minimize the interfacial area excess.

In this communication, we present precise measurements addressed to determine if the capillary interaction force between spherical particles of silica (Bangs Labs, USA), chemically covered by methyl groups, using dichloro dimethyl silane (Sigma-Aldrich, USA), trapped at the A/W interface depends on distance as a r^{-5} power law. These measurements are relevant because there are no precise measurements of the exponent of the power law; most of the time it is used as a convenient assumption, and there is no direct evidence of the corrugation line and the interface distortion in spherical microspheres. Boniello *et al.*[5] using phase-shifting interferometry, where the vertical resolution was enhanced to 1 nm, found no noticeable deformation of the interface in the range of a few micrometers around the bead position trapped at the A/W interface. Despite this, the authors found a relationship between diffusion and particle immersion in terms of thermally activated fluctuations of the interface, at the triple line, driving the system out of mechanical equilibrium and giving extra random forces on the particle. As a consequence of the fluctuation–dissipation theorem, these fluctuating forces induce an extra viscous drag on the particle that leads to a measured diffusion slowing down. Also, with an optical technique, Kaz *et al.*[6] captured the details of a particle approaching an interface, the moment it breaches, and the slow logarithmic time relaxation that follows. The contact line and its undulations move along the

Instituto de Física, Universidad Nacional Autónoma de México, P.O. Box 20-364, México City, 01000, Mexico. E-mail: rolandoc@fisica.unam.mx

† Electronic supplementary information (ESI) available. See DOI: 10.1039/c9sm01051c

particle surface. Therefore, the accompanying interfacial distortion can fluctuate over time. The observed dynamics agree with a model describing activated hopping of the contact line over nanoscale surface heterogeneities, resembling the aging dynamics in glassy systems. As a consequence, colloidal particles trapped at interfaces present novel challenges for understanding their behavior that is not relevant when they are spread in bulk. Some of the inquiries dealing with particles straddling at interfaces include their adsorption,[7,8] equilibrium position and how it is reached,[9] colloidal interactions among them,[3,4,9] self-assembly,[10–12] behavior under shear,[13,14] and applications for systems with particles trapped at interfaces.[15] In this last point, we could include stabilization of large-interface materials, like particle-stabilized emulsions,[16] and bijels,[17,18] or colloidosomes[19] and porous materials,[20] which would be useful to employ interfaces as a scaffold or template to control how colloidal particles self-assemble to make novel materials.

On the A/W interface, the charged functional groups on the submerged colloid surface create an electric double-layer giving rise to an electric dipole that induces dipole repulsion among trapped particles. Park and Furst[21] confirmed the presence of a long-range capillary attraction measuring the effect of the ionic strength on the interaction force between spherical charged colloidal particles, as well as, between colloidal doublets straddling on a decane–water interface using optical tweezers that were calibrated using the particle drag force method. They found that the magnitude and dependence of the attraction on inter-particle distance are consistent with a capillary quadrupole interaction, but the precision was not high enough. In the same interface, Kang *et al.*[22] obtained that the attraction force curve was somewhat consistent with the scaling behavior $F \approx r^{-5}$. Liu *et al.*[23] also found some evidence of this power law during the migration of discs around microposts.

If colloidal particles are made of silica, hydrophobically covered, the electrostatic interactions can be reduced to a minimum. The only remaining interaction comes from capillarity. In our experiment, spherical silica particles ($\zeta_{potential} \sim -25$ mV) chemically covered with dimethylsiloxane of a diameter of 3 μm and 5 μm are trapped at the A/W (Nanopure-UV, resistivity >18.3 MΩ cm) interface, at $T = 23$ °C. The interface with adsorbed particles is in a Langmuir trough equipped with a window, where a 100× objective introduces two beams of a time-sharing optical tweezer from below for trapping the particles. Tweezer separation and swept-frequency are controlled with an acousto-optic deflector driver (ISOMET) (Fig. S1, ESI†). Particle motion is observed and detected using a video camera; particle tracking was performed using standard software. The position of the geometrical center and the force constant of the tweezers, k_i, for each trapped particle, i, in a tweezer must be determined. These parameters are obtained from the particle probability density, $\Psi(r,t)$, by solving the Smoluchowski equation for a particle in Brownian motion urged by the harmonic potential imposed by the optical tweezers. When $t \gg (k/\xi)^{-1} \sim 0.7$ ms, where ξ is the friction constant, $\Psi(r,t)$ for each coordinate is given by:

$$\Psi(x) = \sqrt{k_i/2\pi k_B T}\exp\left\{-\frac{(x-x_0)^2}{2(k_B T/k_i)}\right\}. \qquad (2)$$

The first two moments, μ_1 and μ_2, of the probability distribution of the position fluctuations of the particle give the center position of the tweezer, $x_0 = \mu_1$, and the tweezer force constant, $k_i = k_B T/\mu_2$.

The pair interaction force is directly measured as two straddling particles (i = 1, 2) at the A/W interface, optically trapped, come close to each other. The force between them is obtained by determining the average displacement of the two trapped interacting particles at a distance r, from their corresponding tweezer centers, δx_i (Fig. 1a and b) using a mechanical model

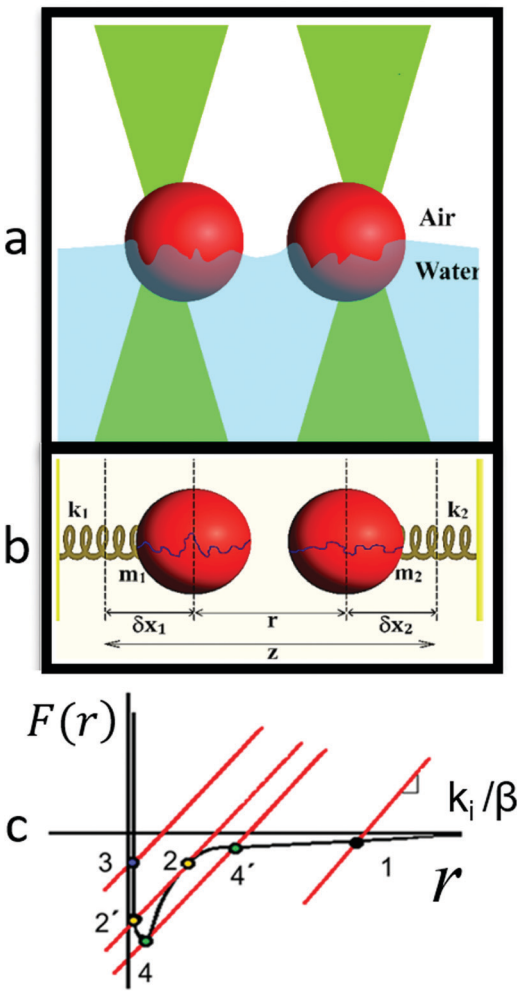

Fig. 1 (a) Two spherical hydrophobic colloidal particles of mass m_i adsorbed at the A/W interface, with a Bond number ≪1, trapped with a time-sharing optical tweezer. The corrugation of the air/water/particle contact line has been exaggerated. (b) Mechanical model: δx_i displacements of particles interacting at distance r from the optical tweezer centers, and the k_i are the force constants of each optical tweezer fixed by the laser power. (c) Drawing of the force–displacement curve. Straight lines represent the effective constant and the black curve the interaction force with a harsh repulsion (contact). Colored dots are mechanical equilibrium points given by the intersection of the lines and the capillary force: 1, 2, 3, 2′, and 4′. When the force gradient is larger than the effective elastic constant, interacting particles become unstable generating discontinuities from which hysteresis follows: the jump-to-contact (2–2′) in the approach curve and the jump-off-contact in the withdrawal curve (4–4′). When the particles make contact, it is not possible to separate them with the tweezers, because adhesion due to the van der Waals force is very strong at contact (Fig. 2c).

(Fig. 1b).[24] Here, the total potential energy of the system is given by $U_T = U(r) + U_1(\delta x_1) + U_2(\delta x_2)$; where $U_i(\delta x_i) = 1/2 k_i \delta x_i$ represents the optical tweezer trapping potentials acting on each particle (i = 1, 2), and $U(r)$ represents the capillary interaction potential for fixed φ_i. The force of the capillary origin is given by $F = -\nabla U(r) = -C/r^n$; C is a fixed constant, n is an unknown exponent, and $r = z - (\delta x_1 + \delta x_2)$; see Fig. 1b. When particles are forced to approach in a stationary way (quasi-static), *i.e.*, $\delta U_T/\delta(\delta x_i) = -\delta U/\delta r + k_i \delta x_i = 0$, this equation ensues: $k_1 \delta x_1 = C/(z - \beta \delta x_1)^n$, where $\beta = (1 + k_1/k_2)$. From that expression or $F/k_i = \delta x_i = C/k_i r^n$, the value of the constants of the potential can be determined by fitting the measured values of δx_i, and r.

The system is in stable equilibrium when: $\delta^2 U_T/\delta(\delta x_i)^2 > 0$, *i.e.*, $k_1/\beta > \partial F/\partial r$. Here k_1/β is an effective force constant. If the force gradient is larger than the effective constant, the system becomes unstable, and particles jump into contact (Fig. 1c). This jump-to-contact discontinuity is equivalent to the jump-to-contact and the jump-off-contact instabilities found in AFM cantilevers that makes it difficult to measure force curves because the effective spring constant is fixed. In our case, changing the power of the laser, we can access different values of the effective constant making it easier to measure the capillary force and the value of n.

It is an unreliable way to proceed to plot the experimental values, supposedly coming from the power-law, in logarithmic scales and fit them by a least squares adjustment to get the constants. We used the reliable method of maximum likelihood,[25] where:

$$n = 1 + k \sum_{i=1}^{k} \ln\left(\frac{x_i}{x_{\min}}\right) \quad \text{and} \quad \sigma = \frac{n-1}{\sqrt{k}}$$

Here, x_i, $i = 1 \ldots n$ are the measured values of x and $x_{\min}$ is the minimum of them, and σ is the statistical expected error. In previous measurements, authors do not mention the use of a method for avoiding statistical bias.

Fig. 2 presents the interaction force between hydrophobic colloidal particles of 3 μm adsorbed at the A/W interface. The points in the graph come from many different values of measured k_i, δx_i, and r, obtained in different experiments. From the fitting curve, we find $n = 5.02 \pm 0.18$ and $C = -26.326 \pm 2.284$ pN μm^5. With these values, the average value for H_2 can be estimated, $H_2 \sim 30$ nm. The inset (b) of Fig. 2 presents the same results for many experiments made on particles of 5 μm; here $n = 5.04 \pm 0.18$. However, here, we did not evaluate C; we just measured n from the experimental values of r and δx_i. The inset (c) of Fig. 2 presents snapshots of a couple of particles in Brownian motion at the interface optically trapped at different distances where r and δx_i are measured.

Our results support the theoretical model of Stamou *et al.*[3] for explaining the origin of the interaction between uncharged colloidal particles trapped at the A/W interface, due to the irregular shape of the contact line. In our case, there is no evidence of electrostatic interaction. Now, a natural step for future research is to measure the interaction between patchy particles trapped at interfaces that are more complex. In particular, Janus

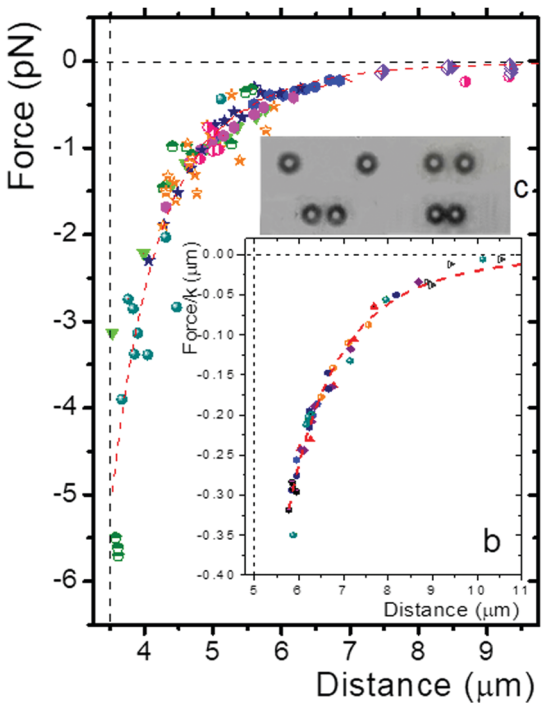

Fig. 2 The capillary interaction force between hydrophobic colloidal particles adsorbed at the A/W interface of a diameter of 3 μm. Inset (b): The same for 5 μm. Inset (c): Snapshots of a couple of particles in Brownian motion at the interface optically trapped at different distances. Different experiments denoted by color.

particles[26] without charge are much more complicated, because the Janus boundary is not necessarily parallel to the interface,[27] and this boundary can be at a different height with respect to the flat interface depending on the Janus balance.[28] The tilted non-equilibrium orientations give rise to inter-particle interactions with a complex angular interaction and a pair potential inversely proportional to the third power of the inter-particle distance (capillary dipolar interaction).[29] The interaction between Janus particles has been estimated using the drag force.[27] However, the thermally activated fluctuations of the interface discussed above are not taken into account, nor the Janus balance and the role of the charge. With our precise measurements, we found that in addition to the quadrupolar interaction, there is a hexapolar contribution. This will be discussed in a forthcoming paper.

Conflicts of interest

There are no conflicts to declare.

Acknowledgements

We acknowledge funds from DGAPA-UNAM (IN106218). We thank S. Ramos and C. Garza for their technical assistance.

References

1 J. F. Joanny and P. G. de Gennes, *J. Chem. Phys.*, 1984, **81**, 552.
2 P. G. de Gennes, *Rev. Mod. Phys.*, 1985, **57**, 827.

3 D. Stamou, C. Duschl and D. Johannsmann, *Phys. Rev. E: Stat. Phys., Plasmas, Fluids, Relat. Interdiscip. Top.*, 2000, **62**, 5263.
4 K. D. Danov, P. A. Kralchevsky, B. N. Naydenov and G. Brenn, *J. Colloid Interface Sci.*, 2005, **287**, 121.
5 G. Boniello, C. Blanc, D. Fedorenko, M. Medfai, N. B. Mbarek, M. In, M. Gross, A. Stocco and M. Nobili, *Nat. Mater.*, 2015, **14**, 908.
6 D. M. Kaz, R. McGorty, M. Man., M. P. Brenner and V. N. Manoharan, *Nat. Mater.*, 2012, **11**, 138.
7 R. W. Style, L. Isa and E. R. Dufresne, *Soft Matter*, 2015, **11**, 7412.
8 N. Ballard, D. Law and S. A. F. Bon, *Soft Matter*, 2019, **15**, 1186.
9 I. B. Liu, N. Sharifi-Mood and K. J. Stebe, *Annu. Rev. Condens. Matter Phys.*, 2018, **9**, 283.
10 R. McGorty, J. Fung, D. Kaz and V. N. Manoharan, *Mater. Today*, 2010, **13**, 34–42.
11 M. Rey, T. Yu, K. Bley, K. Landfester, D. Martin, A. Buzza and N. Vogel, *Langmuir*, 2018, **34**, 9990.
12 A. Kozina, S. Ramos, P. Díaz-Leyva and R. Castillo, *J. Phys. Chem. C*, 2016, **120**, 16879.
13 T. G. Anjali and M. G. Basavaraj, *Langmuir*, 2019, **35**, 3.
14 I. Buttinoni, M. Steinacher, H. T. Spanke, J. Pokki, S. Bahmann, B. Nelson, G. Foffi and L. Isa, *Phys. Rev. E*, 2017, **95**, 012610.
15 V. Lotito and T. Zambelli, *Adv. Colloid Interface Sci.*, 2017, **246**, 217.
16 Y. Yang, Z. Fang, X. Chen, W. Zhang, Y. Xie, Y. Chen, Z. Liu. and W. Yuan, *Front. Pharmacol.*, 2017, **8**, 287.
17 M. F. Haase, K. J. Stebe and D. Lee, *Adv. Mater.*, 2015, **27**, 7065.
18 D. Cai, P. S. Clegg, T. Li, K. A. Rumble and J. W. Tavacoli, *Soft Matter*, 2017, **13**, 4824.
19 K. L. Thompson, M. Williams and S. P. Armes, *J. Colloid Interface Sci.*, 2015, **447**, 217.
20 A. Mohraz, *Curr. Opin. Colloid Interface Sci.*, 2016, **25**, 89.
21 B. J. Park and E. M. Furst, *Soft Matter*, 2011, **7**, 7676.
22 D. W. Kang, K. H. Choi, S. J. Lee and B. J. Park, *J. Phys. Chem. Lett.*, 2019, **10**, 1691.
23 I. B. Liu, G. Bigazzi, N. Sharifi-Mood, L. Yao and K. J. Stebe, *Phys. Rev. Fluids*, 2017, **2**, 100501.
24 B. Capella, G. Dietler, *Surf. Sci. Rep.*, 1999, **34**, 1.
25 M. E. J. Newman, *Contemp. Phys.*, 2005, **46**, 323.
26 L. C. Bradley, W.-H. Chen, K. J. Stebe and D. Lee, *Curr. Opin. Colloid Interface Sci.*, 2017, **30**, 25.
27 B. J. Park, T. Brugarolas and D. Lee, *Soft Matter*, 2011, **7**, 6413.
28 S. Jiang and S. Granick, *J. Chem. Phys.*, 2007, **127**, 161102.
29 H. Rezvantalab and S. Shojaei-Zadeh, *Soft Matter*, 2013, **9**, 3640.

